Narrow Band Gap in La$_{0.8}$MnO$_{2.8}$ as a New Promising Solar Cell Absorber

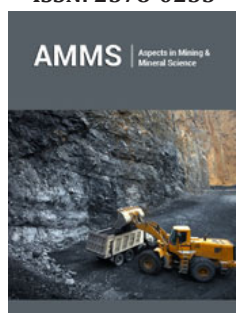**Mabrouki A[1], Bougoffa A[1], Mnasri T[2], Benali A[1,3], Dhahri E[1]* and Valente MA[3]**

[1]Faculty of Sciences of Sfax, University of Sfax, Tunisia

[2]Research Unit UPIM, University of Gafsa, Tunisia

[3]Physics Department, University of Aveiro, Portugal

Abstract

Nanoparticles of manganese oxide La$_{0.8}$MnO$_{2.8}$ were synthesized by the sol-gel method, the oxygen deficiency is created in a controlled manner. The X-ray diffraction measurement proves a coexistence of a minor $Pnma$ orthorhombic phase and a major $R\bar{3}c$ rhombohedral one. The magnetic measurement indicates presents a magnetic transition from a ferromagnetic order to a paramagnetic one at T=232K. In the basis of experimental and the Density Functional Theory (DFT) study, we predicted that the La$_{0.8}$MnO$_{2.8}$ nanoparticles can be considered as a promising solar cell absorber. In fact, DFT calculation proved that this material has a large value of absorption coefficient with a small bandgap E$_g$=1.5eV, which is very close to that of some conventional photovoltaic materials such as Si, CH$_3$NH$_3$PbI$_3$, etc. In addition, the result predicts that this material can be considered a potential candidate in photovoltaic applications.
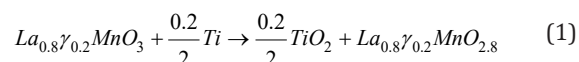
Keywords: Manganite; Oxygen deficiency; Photovoltaic applications; Transport properties

Introduction

In recent years, great interest has been given to manganite oxides thanks to their various proprieties which that make them gaining interest in technological applications (sensor applications, magnetic storage media, solar cell applications...) [1,2]. One of the mean challenges is finding a new ecological material that can be easily synthesized, cheap and non-toxic as a light absorber in photovoltaic applications [3-5]. LaMnO$_3$ is one of the interesting manganite family materials as an antiferromagnetic insulator with trivalent manganese ions (Mn^{3+}). The creation of a vacancy in La sites induces the formation mixed valence which mediate a ferromagnetic interaction between Mn^{3+} and Mn^{4+} cations [6]. Which present the main origin of the physical properties and application fields diversity of this kind of materials. In another hand, DFT calculations present crucial tool alloying to predict the performance of the studied materials. In this work, we mainly focused on the study of the optical properties of La$_{0.8}$MnO$_{2.8}$ material, which presents a very important key to estimate the material optimal performance to the application in solar cells domains [7].

Experimental Procedure

$La_{0.8}\gamma_{0.2}MnO_3$ powder was elaborated using the Sol-Gel as reported in our previous work [1,8]. To create vacancy in oxygen sites with a controller manner, the $La_{0.8}\gamma_{0.2}MnO_3$ compound was placed into a vacuum quartz tubes for at 900 °C for 24j using the titanium as an oxygen absorber according to the following Equation:

$$La_{0.8}\gamma_{0.2}MnO_3 + \frac{0.2}{2}Ti \rightarrow \frac{0.2}{2}TiO_2 + La_{0.8}\gamma_{0.2}MnO_{2.8} \qquad (1)$$

Computational Details

To a successful numerical study $La_{0.8}\gamma_{0.2}MnO_{2.8}$ manganite, we are used the experimental parameters obtained by the DRX refinement. After that, we have created a 2*2*1 super cell contains 19 La, 24 Mn, and 67 O atoms. The ab intio calculations based on the full-potential linearized-augmented plane-wave (FP-LAPW) method as implemented in WIEN2k [9] code

was performed [10]. For the exchange-correlation potential, we employed the Generalized Gradient Approximation (GGA) PBE (Perdew-Burke-Ernzerhof) [11]. The behaviour of the localized Mn 3d electrons is taken in consideration by include the orbital-dependent, on-site Coulomb potential (Hubbard U) $U_{eff}=U-J=4.0eV$ [12]. The integrations in the Brillouin zone are performed on a 5×5×2 grid and the convergence of the Self-Consistent Cycles (SCF) was a considered when the energy difference between them was less than 10^{-4} Ry.

Results and Discussion

The structural refinement of X-ray diffraction pattern using Rietveld method, as displayed in (Figure 1a), shows that $La_{0.8}\gamma_{0.2}MnO_{2.8}$ material presents a coexistence of a minor *Pnma* orthorhombic phase with and a major $R\bar{3}c$ rhombohedral one. The obtained structural parameters are repotted in our previous work [1]. Figure 1b presents the morphology the prepared powder observed by SEM technology proving nanometric particle size. Figure 2 presents the variation of the scaled magnetization as function of temperature. The second derivate of the magnetization (Figure 2) shows that $La_{0.8}\gamma_{0.2}MnO_{2.8}$ material presents a magnetic transition from a ferromagnetic (metallic) order to a paramagnetic (Insulator/Semiconductor) one at T_c=232K when the temperature

increases. Figure 3 proves the total density states obtained using DFT+U calculation showing an asymmetric behavior between the spins up and down states which indicate the magnetic behavior of the studied material [8]. It is clear that the Fermi level is occupied by density levels which indicate the metallic behavior of the studied material. While the spin-down states show a semiconductor behavior. The coexistence of both characteristics proves the semi-metallic behavior of the studied materials [8]. The band structure for the spin-down states (Figure 4) proves a direct energy gap about 1.5eV. Interestingly, this value is very close to thus the Shockley-Queisser band gap of 1.34eV of a single junction solar cell [13]. It is also clear from the (Figure 5) that $La_{0.8}\gamma_{0.2}MnO_{2.8}$ compound has a high light absorption. Therefore, this material could be considered as good candidate for photovoltaic applications. The inset of (Figure 5) presents the Tauc plot. We notice that the optical band gap in z direction is the same as the electronic band gap. However, we notice the existence of an optical anisotropy between xx and zz directions. In order to understand the transport mechanism in this material, we calculated the electrons and holes effective mass (m_e^* and m_h^*) using a polynomial fit of the minimum and maximum of B.C and B.V, respectively using the following relation.

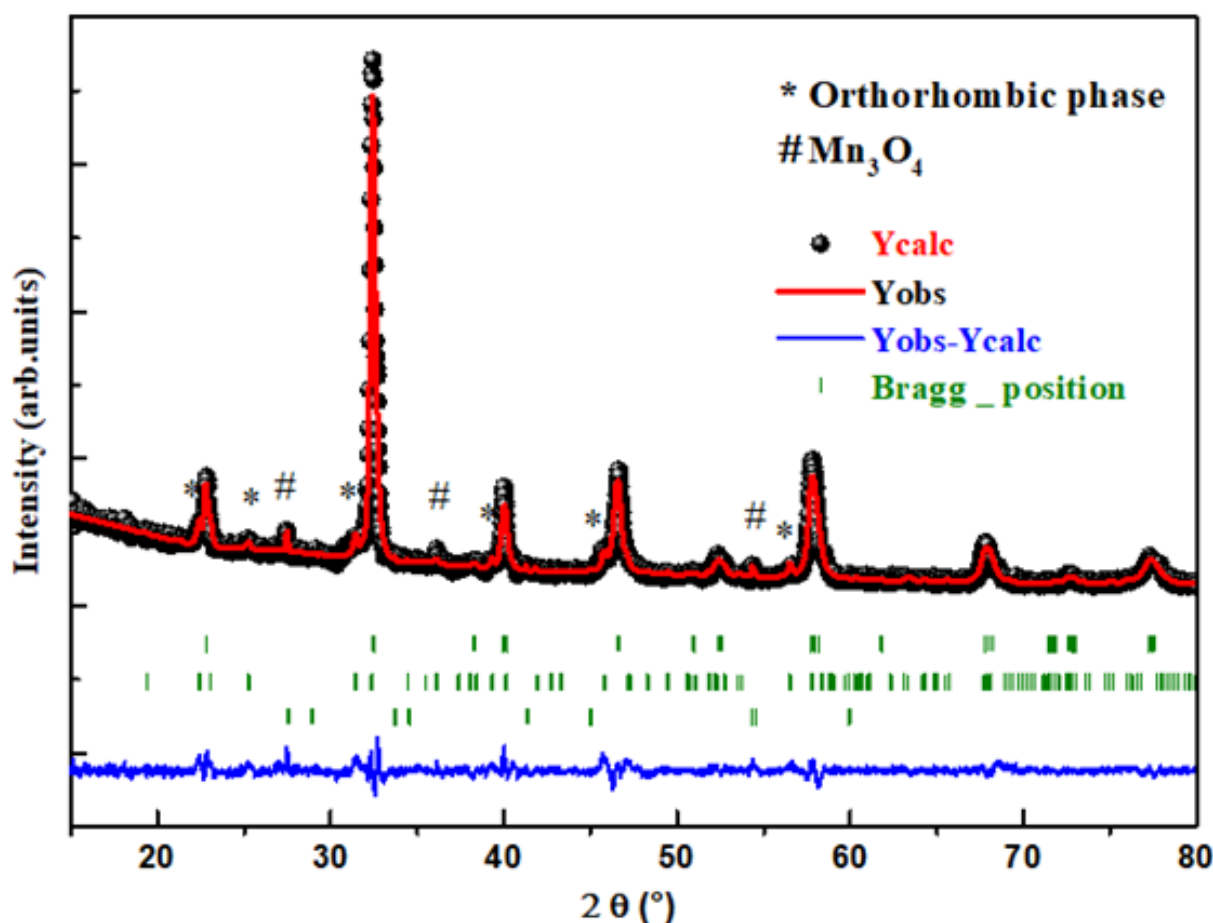$$m^* = h^2 \left(\frac{\partial^2 E}{\partial k^2}\right)^{-1} \quad (2)$$

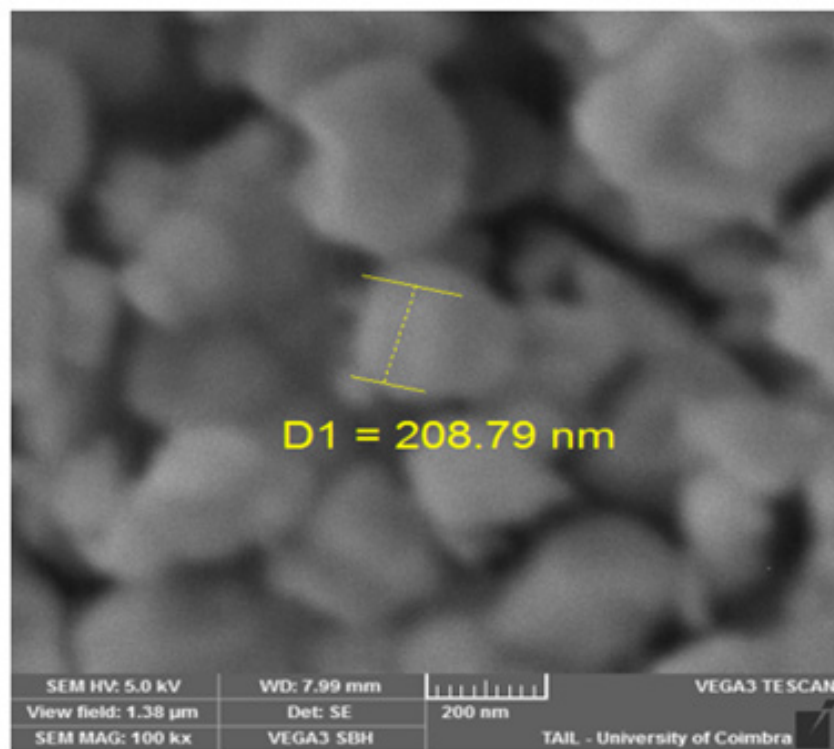**Figure 1a:** Rietveld refinement for $La_{0.8}\gamma_{0.2}MnO_{2.8}$ sample.

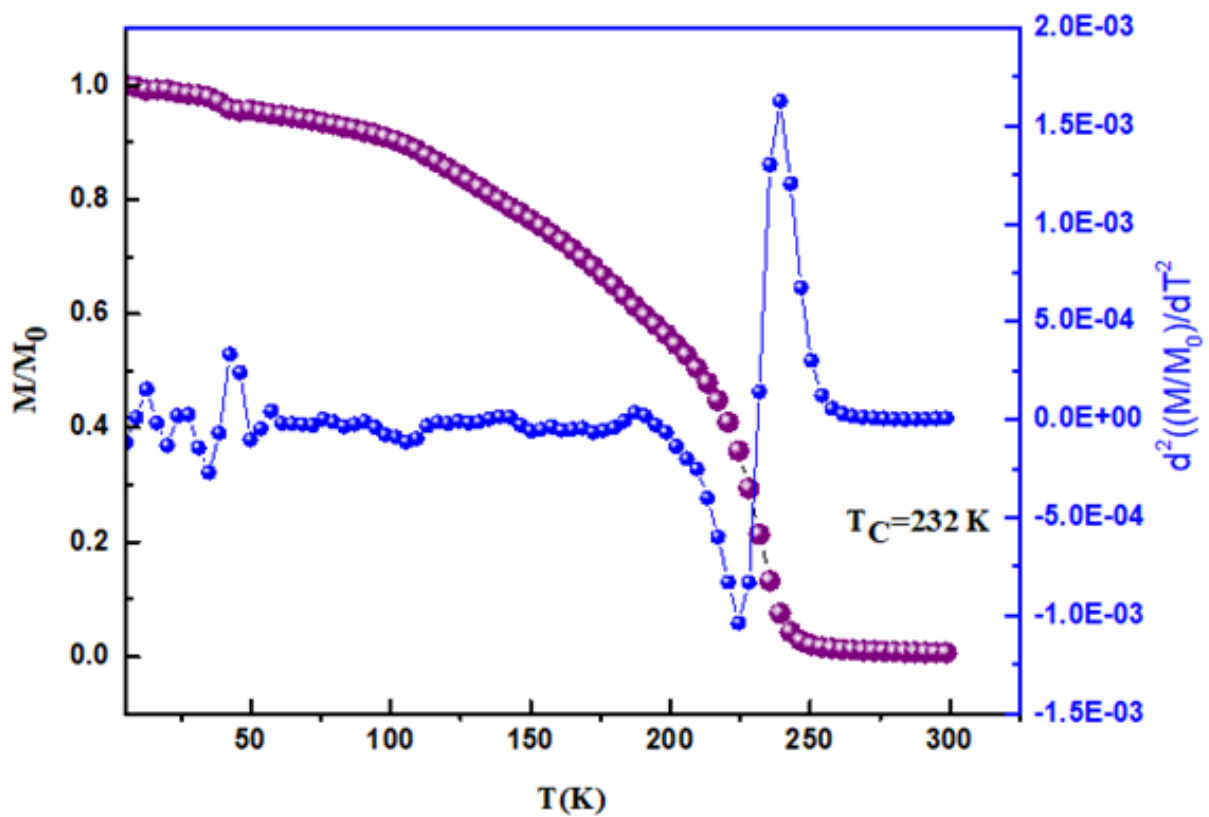**Figure 1b:** SEM image for $La_{0.8}\gamma_{0.2}MnO_{2.8}$ sample.

Figure 2: The temperature dependence of the magnetization, the inset presets the second derivate of the magnetization as function of temperature.
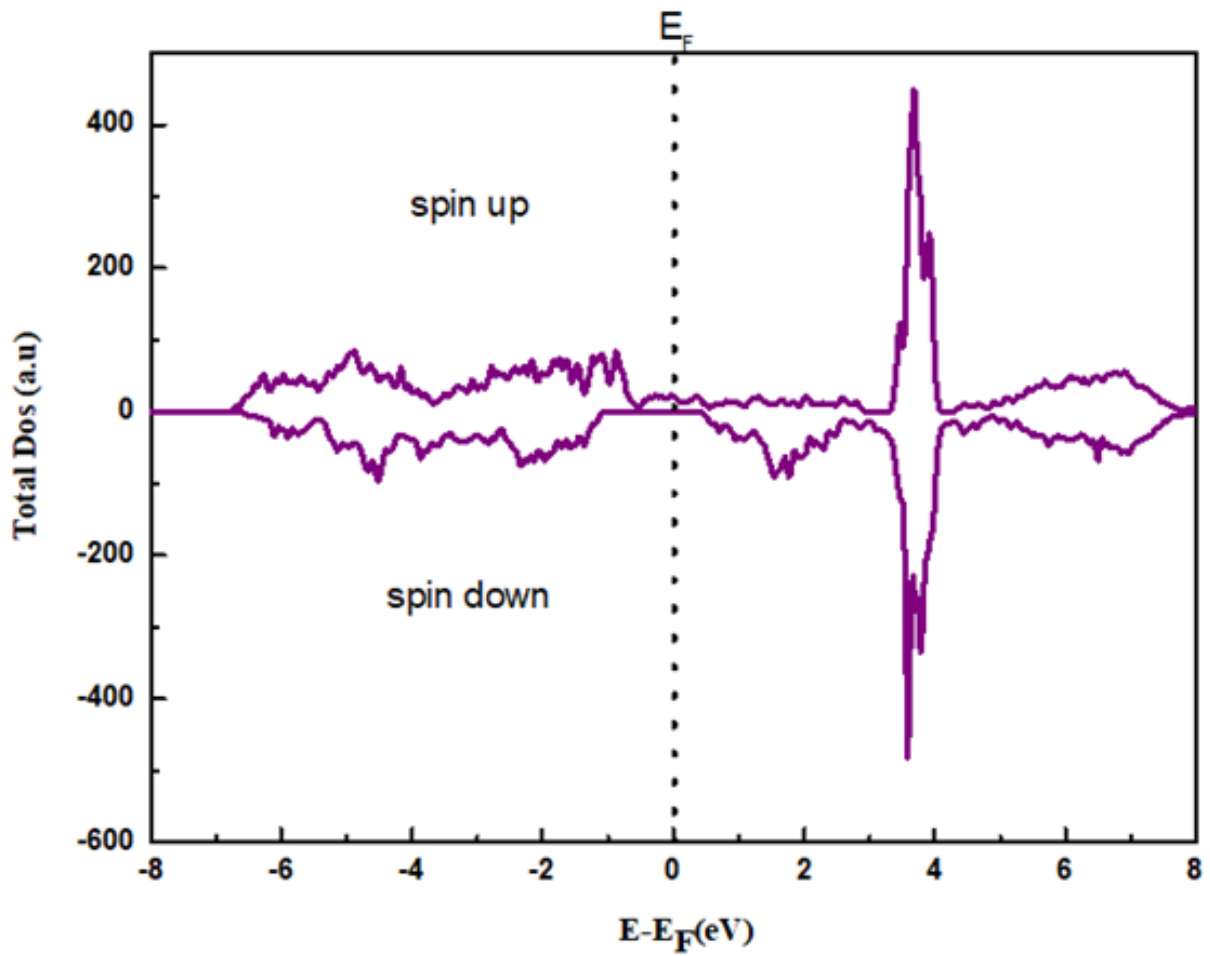
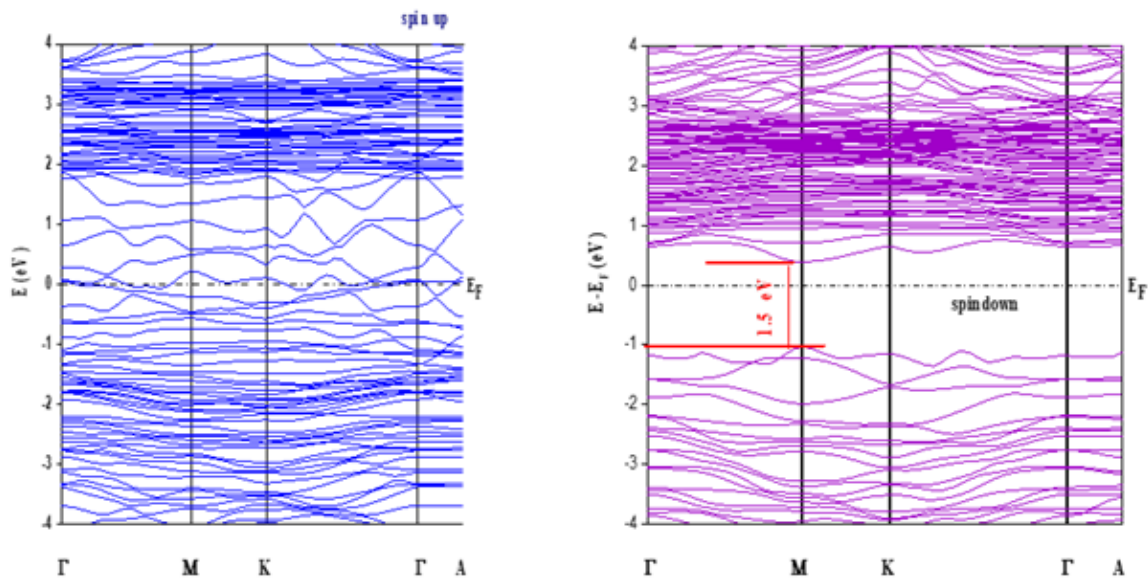**Figure 3:** The total density of state for $La_{0.8}\gamma_{0.2}MnO_{2.8}$ sample.

Figure 4: Majority (up) and minority (down) spin band structures of $La_{0.8}\gamma_{0.2}MnO_{2.8}$.
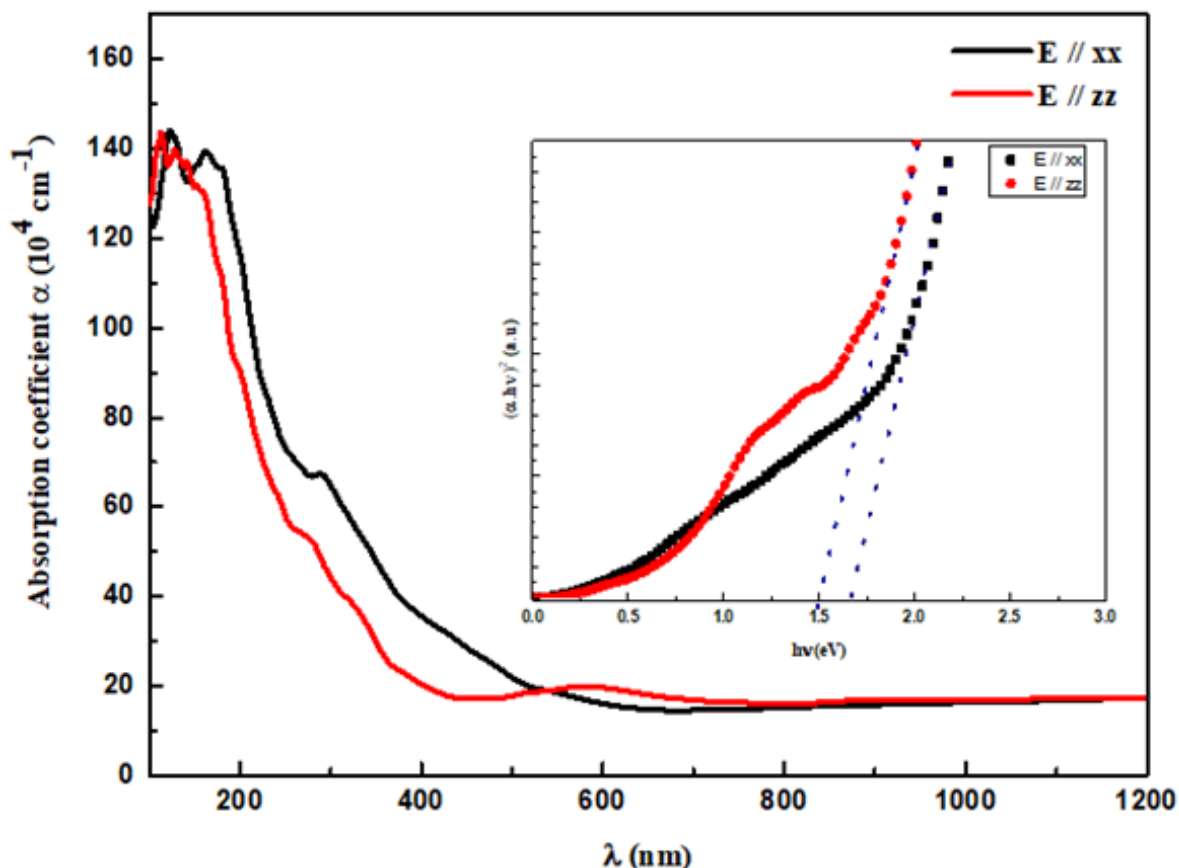
Figure 5: The variation of the absorption coefficient as a function of the wavelength, the inset shows the Tauc plot.

The obtained values are m_e*=2.54 m_0 and m_h*=0.892 m_0. So, we can calculate the electron and hole thermal velocity V_{th} using this relation:

$$V_{th} = \sqrt{\frac{3k_B T}{m^*_{e/h}}} \quad (3)$$

We obtain V_{th}=7.326*10^4m/s and 1.236*10^5m/s for electrons and holes, respectively.

The electron and holes density can be calculate using the following relations [14]:

$$n = 2\frac{\left(2\pi m_e^* k_B T\right)^{3/2}}{h^3} \exp\left(-\frac{E_c - E_F}{k_B T}\right) \quad (4)$$

$$p = 2\frac{\left(2\pi m_p^* k_B T\right)^{3/2}}{h^3} \exp\left(\frac{E_V - E_F}{k_B T}\right) \quad (5)$$

The obtained parameters are summarized in Table 1. We found then: n=4.11*10^{11}cm^{-3} and p=3.47*10^8cm^{-3}. The holes density is negligible to the electrons one, which suggests that the material, in spin down states, is an n-type semiconductor.

Table 1: Band gap and transport properties.

M_e*/m_0	M_p*/m_0	V_{th} (e) (m/s)	V_{th} (h) (m/s)	N_c (cm^{-3})	N_v (cm^{-3})	n (cm^{-3})	P (cm^{-3})	E_g (e.V)
2.54	0.89	7.326*10^4	1.236*10_5	1.015*10^{20}	2.113*10^{19}	4.11*10^{11}	3.47*10^8	1.5

Conclusion

To sum up, the $La_{0.8}\gamma_{0.2}MnO_{2.8}$ synthesized by Sol-Gel route shows a coexistence of a minor *Pnma* orthorhombic phase and a major $R\bar{3}c$ rhombohedral one. The DFT calculation exhibits that the prepared nanoparticles present a wide absorption with a narrow band gap witch make this material considered as potential candidate to the photovoltaic applications.

Acknowledgement

References

1. Mabrouki A, Benali T, Mnasri E, Dhahri E, Valente J (2020) Oxygen deficiency effect on the magnetocaloric and critical phenomena for $La_{0.8}\square_{0.2}MnO_{3-\Delta}$ (Δ=0, 0.1 and 0.2) compounds: Significant enhancement of relative cooling power. Mater Sci: Mater Electron 31: 22749-22767.

2. Sheikh M, Sakhya A, Maity R, Dutta A, Sinha TP (2019) Narrow band gap and optical anisotropy in double perovskite oxide Sm_2NiMnO_6: A new promising solar cell absorber. Sol Energy Mater Sol Cells 193: 206-213.

3. Zhao XG, Yang JH, Fu Y, Yang D, Xu Q, et al. (2017) Design of lead-free inorganic halide perovskites for solar cells via cation-transmutation. J Am Chem Soc 139(7): 2630-2638.

4. Grinberg I, West DV, Torres M, Gou G, Stein DM, et al. (2013) Perovskite oxides for visible-light-absorbing ferroelectric and photovoltaic materials. Nature 503(7477): 509-512.

5. Das S, Bhattacharya RN, Mandal KC (2016) Performance limiting factors of $Cu_2ZnSn(S_xSe_{1-x})_4$ solar cells prepared by thermal evaporation. Sol Energy Mater Sol Cells 144: 347-351.

6. Marouani Y, Gharbi S, Issaoui F, Dhahri E, Costa BFO, et al. (2020) Magneto-transport properties of the Ag doping Sr site in $La_{0.57}Nd_{0.1}Sr_{0.33-x}Ag_xMnO_3$ (0.00 and 0.15) manganites. Low Temp Phys 200: 131-141.

7. Omata T, Nagatani H, Suzuki I, Kita M, Yanagi H, et al. (2014) Wurtzite $CuGaO_2$: A new direct and narrow band gap oxide semiconductor applicable as a solar cell absorber. J Am Chem Soc 136(9): 3378-3381.

8. Mabrouki A, Mnasri T, Bougoffa A, Benali A, Dhahri E, et al. (2021) Experimental study and DFT calculation of the oxygen deficiency effects on structural, magnetic and optical properties of $La_{0.8}\square_{0.2}MnO_{3-\delta}$ (δ=0, 0.1 and 0.2) compounds. J Alloys Compd 860: 157922.

9. Blaha P, Schwarz K, Madsen GKH, Kvasnicka D, Luitz J (2001) WIEN2K, an augmented plane wave+local orbitals program for calculating crystal properties. Karlheinz Schwarz, Technical University, Wien, Austria.

10. Hohenberg P, Kohn W (1964) Inhomogeneous electron gas. Phys Rev B 136: 864.

11. Kresse G, Hafner J (1994) Ab initio molecular-dynamics simulation of the liquid-metal-amorphous-semiconductor transition in germanium. Phys Rev B 49(20): 14251-14269.

12. Wang L, Maxisch T, Ceder G (2006) Oxidation energies of transition metal oxides within the GGA+U framework. Phys Rev B 73: 195107.

13. Tauc J, Grigorovici R, Vancu A (1966) Optical properties and electronic structure of amorphous germanium. Phys Status Solidi 15(2): 627-637.

14. Liu J, Jiang QY, Zhang S, Zhang H (2019) Carrier mobility and relaxation time in BiCuSeO. Phys Lett 383(34): 125990.

For possible submissions Click below:

Submit Article